

Damping of spin waves and singularity of the longitudinal modes in the dipolar critical regime of the Heisenberg ferromagnet EuS

P. Böni

Physik-Department E21, Technische Universität München, D-85748 Garching, Germany
and Laboratory for Neutron Scattering ETH & PSI, CH-5232 Villigen PSI, Switzerland

B. Roessli

Institut Laue Langevin, F-38042 Grenoble, France
and Laboratory for Neutron Scattering ETH & PSI, CH-5232 Villigen PSI, Switzerland

D. Görlitz and J. Kötzler*

Institut für Angewandte Physik und Zentrum für Mikrostrukturforschung, D-20355 Hamburg, Germany
(Received 18 October 2001; revised manuscript received 4 January 2002; published 2 April 2002)

By inelastic scattering of polarized neutrons near the (200) Bragg reflection, the susceptibilities and linewidths of the spin waves and the longitudinal spin fluctuations, $\delta\mathbf{S}_{sw}(\mathbf{q})$ and $\delta S_z(\mathbf{q})\|\mathbf{M}_s$, respectively, were determined separately. By aligning the momentum transfers \mathbf{q} perpendicular to both $\delta\mathbf{S}_{sw}$ and the spontaneous magnetization \mathbf{M}_s , we explored the statics and dynamics of these modes with transverse polarizations with respect to \mathbf{q} . In the dipolar critical regime, where the inverse correlation length $\kappa_z(T)$ and q are smaller than the dipolar wave number q_d , we observe that (i) the static susceptibility of $\delta\mathbf{S}_{sw}(\mathbf{q})$ displays the Goldstone divergence while for $\delta S_z(\mathbf{q})$ the Ornstein-Zernicke shape fits the data with a possible indication of a thermal (mass) renormalization at the smallest \mathbf{q} values; i.e., we find indications for the predicted $1/q$ divergence of the longitudinal susceptibility; (ii) the spin-wave dispersion as predicted by the Holstein-Primakoff theory revealing $q_d=0.23(1) \text{ \AA}^{-1}$, in good agreement with previous work in the paramagnetic and ferromagnetic regime of EuS; (iii) within experimental error, the (Lorentzian) linewidths of both modes turn out to be identical with respect to the q^2 variation, the temperature independence, and the absolute magnitude. Due to the linear dispersion of the spin waves, they remain underdamped for $q < q_d$. These central results differ significantly from the well-known exchange-dominated critical dynamics, but are quantitatively explained in terms of dynamical scaling and existing data for $T \geq T_C$. The available mode-mode coupling theory, which takes the dipolar interactions fully into account, describes the gross features of the linewidths but not all details of the T and \mathbf{q} dependences.

DOI: 10.1103/PhysRevB.65.144434

PACS number(s): 75.40.Gb, 68.35.Rh

I. INTRODUCTION

Neutron scattering has been demonstrated as an extremely useful probe of the spin fluctuations $\delta\mathbf{S}(\mathbf{q})$ near the Curie temperature of Heisenberg ferromagnets.¹⁻⁴ Under the assumption that the *isotropic exchange interaction* dominates the ordering process, the early results could be well interpreted in terms of the dynamical scaling hypothesis.⁵ In its simplest form this hypothesis states that as for the static spin correlations also the temperature and \mathbf{q} dependences of their characteristic frequencies are described by homogeneous scaling functions that depend only on a single variable $q\xi(T)$, where ξ denotes the correlation length of the order parameter fluctuations and $q=|\mathbf{q}|$.

Signatures of the inevitable, *anisotropic dipole-dipole interaction* on the fluctuations of Heisenberg ferromagnets have been first detected by measurements of the relaxation rate $\Gamma(0)$ of the homogeneous $\delta S(0)$ mode in the *paramagnetic* phase of CdCr_2Se_4 (Ref. 6) and subsequently also of Fe by neutron spin-echo measurements at small \mathbf{q} .⁷ Based on these signatures and also on first theoretical approaches, which treated the dipolar interaction as a perturbation of the isotropic fluctuations,^{8,9} it has been conjectured¹⁰ that the

dipolar forces should gain importance somewhere in the so-called dipolar critical (DC) regime, where $\xi^{-1} \equiv \kappa$ and q are small compared to the dipolar wave number q_d [see Fig. 1(a)]. For a given ferromagnet, this quantity measures the strength of the dipolar interaction relative to the exchange interactions. It has been introduced in renormalization group (RG) calculations of the static correlation functions,¹¹ recognizing that the dipolar anisotropy breaks the rotational invariance of the fluctuations $\delta\mathbf{S}(\mathbf{q})$ with respect to \mathbf{q} . The demagnetizing effect of the dipolar interaction on the longitudinal modes $\delta S_z\|\mathbf{q}$ prevents them from becoming critical, while the remaining two transverse modes [see Fig. 1(c)] are driving the ferromagnetic transition. At first these dipolar anisotropic fluctuations have been realized by elastic scattering of polarized neutrons above T_C of the Heisenberg ferromagnets EuO and EuS,¹² where for the latter it was also possible to measure directly the characteristic wave number, $q_d=0.22(5) \text{ \AA}^{-1}$.

On the theoretical side, the implications of the dipolar critical fluctuations on their dynamics have been fully taken into account only by the mode-mode coupling (MMC) approach.¹³⁻¹⁶ Above T_C , rather convincing agreement was obtained^{13,14} for the critical slowing down of $\Gamma^\alpha(\mathbf{q})$ observed for $q \rightarrow 0$ and $T \rightarrow T_C$ on the transverse fluctuations of Fe

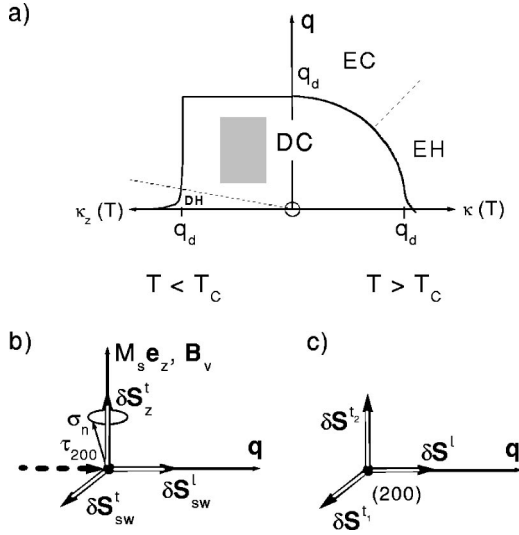


FIG. 1. (a) Dipolar regime for static critical behavior below T_C explored in the present work (shaded area), with $q_d = 0.23 \text{ \AA}^{-1}$ for EuS. The dotted lines define the exchange (EH) and dipolar (DH) hydrodynamic critical regimes above and below T_C , respectively. (b) Spin fluctuation modes defined by the geometry of our polarized neutron experiment below T_C of EuS, where the momentum transfer $\mathbf{q} = \mathbf{Q} - \boldsymbol{\tau}_{200}$ is kept perpendicular to the spontaneous magnetization. Spin-wave ($\delta\mathbf{S}_{sw}$) and longitudinal ($\delta\mathbf{S}_z$) fluctuations are detected separately by the spin-flip and non-spin-flip intensities for neutrons with incident polarization $\boldsymbol{\sigma}_n$ and wave vector \mathbf{Q} . (c) Definition of the magnetic modes with respect to the reduced momentum transfer \mathbf{q} .

(Ref. 7) and EuS (Ref. 17) as well as for the longitudinal ones ($\alpha=L$) of EuS.¹⁷ Additional strong support for the MMC results came from quantitative analyses of the relaxation rates $\Gamma^l(\mathbf{q}, T)$ in the two limiting cases $q=0, T \geq T_C$ and $T=T_C, q \geq 0$ for the archetype Heisenberg ferromagnets.¹⁸ As one of the striking results we mention the crossover from $\Gamma^l(q > q_d, T_C) \sim q^{5/2}$ in the exchange-dominated regime to $\Gamma^l(q \ll q_d, T_C) \sim q^2$, deep in the dipolar one.^{7,13,14} The latter behavior corresponds to the conventional (van Hove type) slowing down, characterized by a noncritical Onsager coefficient of the spin dynamics, $L^l(\mathbf{q}, T) \equiv \Gamma^l(\mathbf{q}) \cdot \chi^l(\mathbf{q})$,^{13,14,18} where $\chi^l(\mathbf{q})$ is the static susceptibility of the transverse fluctuations. It was shown that this central quantity depends in a universal manner only on T_C and q_d , to be discussed in Sec. V.

Below T_C , the situation becomes more complicated because the symmetry of the fluctuations is further reduced by the appearance of the order parameter, i.e., the spontaneous magnetization \mathbf{M}_s . As illustrated in Fig. 1(b), it is common sense to distinguish there between the spin waves $\delta\mathbf{S}_{sw}(\mathbf{q}) \perp \mathbf{M}_s \mathbf{e}_z$ and the longitudinal modes $\delta\mathbf{S}_z(\mathbf{q}) \parallel \mathbf{M}_s \mathbf{e}_z$. A systematic classification of critical behaviors in the q - $\kappa(T)$ plane, which considers the Heisenberg exchange and the dipolar interaction on an equal footing, has recently been performed by Schinz and Schwabl.¹⁹ According to their results, we have depicted the DC regime in Fig. 1(a), which apart from a dipolar hydrodynamic (DH) regime at rather small q is bound from above by the dipolar wave number q_d in the q

direction as well as in the $\kappa_z(T)$ direction.

Since among the archetypical Heisenberg ferromagnets q_d is largest for EuS,^{10,18} this material is preferred for experimental studies of dipolar effects.^{12,17,20–22} Here we report results of a systematic study of the magnetization dynamics in the DC region, which covers the shaded area in Fig. 1(a). Our principal goal is to determine the susceptibilities and linewidths of the spin waves and of the longitudinal fluctuations and to examine their \mathbf{q} and temperature variations. The experimental access by means of inelastic scattering of polarized neutrons around a finite Bragg peak is described in Sec. II. As illustrated by Fig. 1(b) we choose a configuration where the momentum transfer \mathbf{q} occurs in directions perpendicular to the order parameter \mathbf{M}_s , which allows us to define and determine the transverse polarizations of the spin wave and of the longitudinal modes with respect to \mathbf{q} . This will turn out to be essential for the discussion by means of dynamical scaling, because the appearance of the order parameter does not lift the symmetry with respect to \mathbf{q} so that both modes retain their transverse polarization from above T_C . In Sec. III, we give some examples for constant \mathbf{Q} scans and the analysis of the inelastic cross section. We evaluate there the relevant observables, i.e., static susceptibilities, spin-wave frequencies, and linewidths. Their detailed temperature and \mathbf{q} variations are presented in Sec. IV. In particular, we determine there the dipolar wave number q_d from spin-wave energies and the correlation length $\xi(T) = \kappa_z^{-1}(T)$ of the longitudinal fluctuations from their static susceptibilities. Backed by these findings, we discuss the central results, i.e., the damping of the spin waves and of the longitudinal fluctuations, in Sec. V. Here the objectives are twofold. First, basing on the existing data for the paramagnetic side of EuS we want to examine whether and how the scaling hypothesis, which is rather special for the dipolar interaction,⁵ works, and second we will compare our results to the rather detailed predictions of recent numerical solutions of the MMC equations.¹⁶ To produce explicit values for the linewidth, this MMC approach had to introduce several assumptions which, of course, need to be checked by experiment. The paper closes with a brief summary and outlook.

II. EXPERIMENT

The neutron scattering experiments were performed using the triple-axis spectrometer IN14 at the ILL in Grenoble, with polarization analysis. The isotopically enriched sample ¹⁵³EuS was composed of roughly 100 single crystals, aligned such that the overall mosaic was $\eta \approx 0.75^\circ$ (see Fig. 2). A small mosaic is of the utmost importance to allow measurements as close to the Bragg peak as possible. In EuS the magnetic Eu^{2+} ions ($S=7/2, g_L=2$) are arranged on a face-centered cubic lattice, $a_0 = 5.973 \text{ \AA}$. The sample was mounted inside a superconducting magnet providing vertical fields B_v up to 4.5 T. All measurements were conducted near the (200) Bragg peak with \mathbf{q} along the $[h00]$ direction [see Fig. 1(b)] using neutrons with fixed incident energies $E_i = 3.0$ and 3.8 meV and collimations $37' - 37' - 40'$ along the beam direction from the monochromator to the detector. Due to the mosaic structure of the sample shown in Fig. 2, the

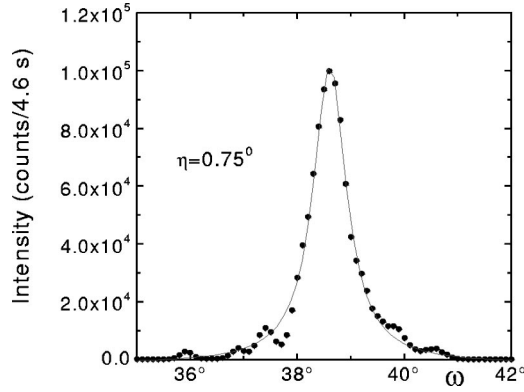


FIG. 2. Rocking curve of the τ_{200} Bragg peak of the isotopically enriched sample ^{153}EuS that is composed of more than 100 individual single crystals. The mosaic of the sample is $\eta = 0.75^\circ \pm 0.02^\circ$.

measurements in the other \mathbf{q} direction suffered from a high background from the elastic Bragg intensity.

The neutron cross section for neutrons scattered from an isotropic magnetic material is given by²³

$$\frac{d^2\sigma}{d\Omega dE'} = \frac{k_f}{k_i} \left(\frac{\gamma r_0}{2} \right)^2 NF(\mathbf{Q})^2 \exp[-2W(\mathbf{Q})] \times \sum_{\alpha\beta} (1 - \hat{Q}_{\alpha\beta}^2) S_{\alpha\beta}(\mathbf{q}, \omega). \quad (1)$$

$\mathbf{Q} = \mathbf{k}_i - \mathbf{k}_f$ and $\hbar\omega = E_i - E_f$ are the total momentum and energy transfers from the neutron to the sample, respectively, where $E_{i,f} = (\hbar k_{i,f}^2 / (2m_n))$ is the neutron energy. α and β designate the Cartesian components x, y, z , $(\gamma r_0 / 2)^2 = 72.65 \times 10^{-3} \text{ b} / \mu_B^2$, F is the magnetic form factor for the Eu^{2+} ion, the exponential term is the Debye-Waller factor, $\hat{\mathbf{Q}} = \mathbf{Q} / |\mathbf{Q}|$, and N is the number of magnetic ions in the sample. The reduced momentum transfer is defined by $\mathbf{q} = \mathbf{Q} - \boldsymbol{\tau}_{200}$, where $\boldsymbol{\tau}_{200}$ is the position of the nearest Bragg peak, $\boldsymbol{\tau}_{200} = (200)2\pi/a_0$ in our case [Fig. 1(b)].

The $\alpha\beta$ component of the scattering function $S_{\alpha\beta}(\mathbf{q}, \omega)$ is related to the imaginary part of the susceptibility by the fluctuation-dissipation theorem:

$$S_{\alpha\beta}(\mathbf{q}, \omega) = \langle n + 1 \rangle \frac{1}{\pi} \text{Im} \chi_{\alpha\beta}(\mathbf{q}, \omega),$$

where the thermal population factor is given by $\langle n \rangle = [\exp(\hbar\omega/k_B T) - 1]^{-1}$. Our experiments have been conducted close to the Curie temperature $T_C = 16.25 \text{ K}$ and at energy transfers $\hbar\omega \ll k_B T$, so that $S_{\alpha\beta}$ becomes directly proportional to $T \text{Im} \chi_{\alpha\beta}$:

$$S_{\alpha\beta}(\mathbf{q}, \omega) = \frac{k_B T}{\hbar\omega} \frac{1}{\pi} \text{Im} \chi_{\alpha\beta}(\mathbf{q}, \omega). \quad (2)$$

Thus, the neutron scattering cross section reflects directly the \mathbf{q} and ω dependences of the susceptibility components of the sample.

According to Eq. (1), the neutrons couple only to spin fluctuations $\delta\mathbf{S}$ that are perpendicular to the scattering vector $\mathbf{Q} = \boldsymbol{\tau}_{200} + \mathbf{q}$. Therefore, the cross section contains contributions from the longitudinal fluctuations δS_z^t and from the spin-wave scattering that corresponds to excitations with $\delta\mathbf{S}_{sw}^t$ perpendicular to \mathbf{M} . Both modes have a transverse polarization with respect to \mathbf{q} , and in the following we omit the superscript t . The fluctuations parallel to \mathbf{M} can be separated from the spin-wave modes by analyzing the polarization $\boldsymbol{\sigma}_f = \pm \boldsymbol{\sigma}_i$ of the scattered neutrons with respect to the incident polarization, $\boldsymbol{\sigma}_i \parallel \mathbf{B}_v$. As can be inferred from Fig. 1(b), the parallel fluctuations give rise to non-spin-flip scattering and the spin-wave modes give rise to spin-flip scattering. Therefore, the susceptibilities $\chi_z(\mathbf{q}, \omega)$ and $\chi_{sw}(\mathbf{q}, \omega)$ of both magnetic modes can be determined unambiguously in a vertical field \mathbf{B}_v .

Because of the depolarization of the neutron beam by the orientational averaging of the magnetic domains we conducted most measurements in a vertical field $30 \text{ mT} < B_v < 45 \text{ mT}$. This value was large enough to ensure a reasonable polarization of the beam, but yet sufficiently small to minimize the influence of the internal magnetic field $\mathbf{B} = \mathbf{B}_v - N_z \mathbf{M}(T)$ (with $N_z = 0.05$; see Ref. 21) on the spin fluctuations as much as possible.

In a first step, all the measured data $I_{\text{obs}}^{\mu\nu}$ was corrected for the finite flipping ratio R according to

$$I_z = \frac{R}{R-1} I_{\text{obs}}^{++} - \frac{1}{R-1} I_{\text{obs}}^{+-},$$

$$I_{sw} = \frac{R}{R-1} I_{\text{obs}}^{+-} - \frac{1}{R-1} I_{\text{obs}}^{++},$$

where $I^{\mu\nu}$ designates the scattered intensity from the polarization μ to the polarization ν of the incident and scattered neutrons, respectively. In a second step, a background being determined in the paramagnetic phase at $T = 80 \text{ K} \gg T_C$ and in the ordered phase at $T = 1.78 \text{ K}$ was subtracted from the data. The energy-independent contribution was 1 count/8.3 min for all the measurements in the range $0.06 < \zeta < 0.18$,^{24,25} where the reduced momentum transfer is measured in reciprocal lattice units $\zeta = q / (2\pi/a_0)$. The peak intensity of the elastic background was 4 counts/8.3 min and 8 counts/min for the spin-flip and non-spin-flip scattering at the position $\boldsymbol{\tau} + \mathbf{q}$, respectively.

III. CONSTANT-Q SPECTRA

The inelastic magnetic scattering has been determined at several temperatures and momentum transfers by performing constant- \mathbf{Q} scans. Figure 3 shows the cross sections at $\zeta = 0.18$ as measured along the $[100]$ direction at the $(2\ 0\ 0)$ Bragg reflection at $T = 15 \text{ K}$ in a field $B_v = 100 \text{ mT}$. The spin-flip data clearly reveal spin waves, while the non-spin-flip data are quasielastic and have a width (half width at half maximum) that is roughly a factor of 2 smaller than the energy of the spin waves. Similar data were collected for many different temperatures $1.78 \leq T \leq 80 \text{ K}$ and in appropriate fields $30 \text{ mT} \leq B_v \leq 500 \text{ mT}$, as described in Sec. II.

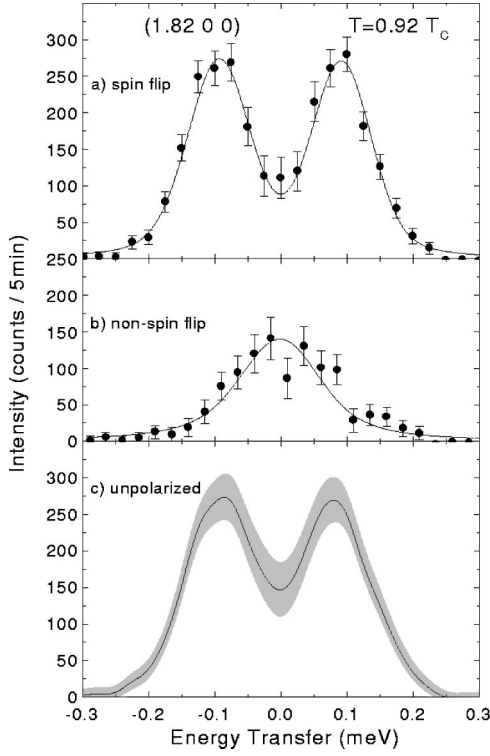


FIG. 3. Constant- \mathbf{Q} scans for (a) spin-flip and (b) non-spin-flip neutrons scattered from spin-wave and longitudinal fluctuations, respectively, at $T=0.92T_C=15.0$ K. (c) Spectrum for unpolarized neutrons, calculated from (a) and (b), showing the depression of the longitudinal contribution.

Scattering of polarized neutrons is a very efficient way to properly separate the longitudinal from the transverse excitations in a Heisenberg ferromagnet. This is demonstrated in Fig. 3(c) where we show for comparison the spectrum calculated from the (flip efficiency) corrected intensities of Figs. 3(a) and 3(b):

$$I_{unpol}(\omega) = \frac{2}{3}I_{sw}(\omega) + \frac{1}{3}I_z(\omega),$$

as would be measured by means of unpolarized neutrons. The comparison shows clearly that the longitudinal scattering cannot be reliably extracted by means of unpolarized neutrons because the spectral widths of I_{sw} and I_z are similar. Moreover, reliable positions and widths of the spin waves can only be obtained if polarized beam data are used.

In order to analyze the data we have employed the scattering function, Eq. (1), which via Eq. (2) is directly related to the dynamical susceptibilities χ_z and χ_{sw} . To allow for a comparison between our results and the existing theory,¹³ we assume Lorentzian spectral weight functions for the dynamic susceptibilities of the modes $\mu=z,sw$ and obtain

$$\text{Im}[\chi_\mu(\mathbf{q},\omega)] = \chi_\mu(\mathbf{q}) \frac{1}{2\pi} \left(\frac{\hbar\omega\Gamma_\mu}{[\omega - \omega_\mu(\mathbf{q})]^2 + (\Gamma_\mu)^2} + \frac{\hbar\omega\Gamma_\mu}{[\omega + \omega_\mu(\mathbf{q})]^2 + (\Gamma_\mu)^2} \right), \quad (3)$$

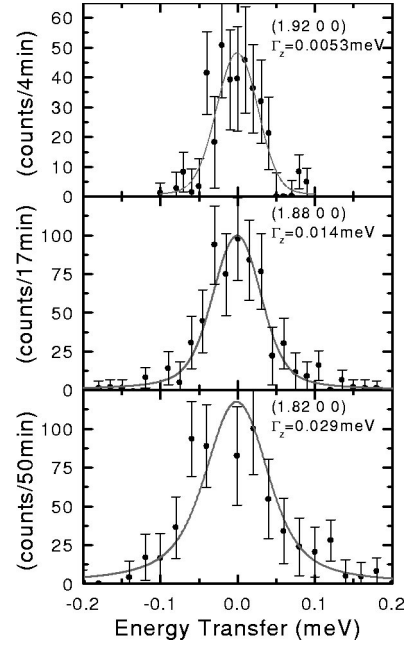


FIG. 4. Spectra of the longitudinal fluctuations recorded at $T=0.96T_C$ and different momentum transfers \mathbf{q} .

where $\hbar\omega_{sw} \equiv E_{sw}(\mathbf{q})$ is the spin-wave energy and $\Gamma_\mu(\mathbf{q})$ are the linewidths. As the scattering from the longitudinal fluctuations proves to be quasielastic, we set $\omega_z(\mathbf{q})=0$. The data were fitted by convoluting the scattering functions $S_\mu(\mathbf{q},\omega)$ with the four-dimensional resolution function of the spectrometer to give $I_\mu(\mathbf{q},\omega)$. The three parameters E_{sw} , Γ_μ , and $\chi_\mu(\mathbf{q})$ and a common normalization parameter were varied for each constant- \mathbf{Q} scan such that χ^2 was minimized. The solid lines in Figs. 3(a) and 3(b) are fits to the data using Eq. (3). They describe the data well. Figures 4 and 5 show that the width of the longitudinal fluctuations Γ_z increases with increasing q in qualitative agreement with existing theories.^{5,8,14} A more detailed comparison will be performed in the discussion.

IV. ANALYSIS OF THE SPECTRA

From the fits of the spectra using the double Lorentzian scattering function, Eq. (3), as described in the previous paragraph, we extracted the static susceptibilities $\chi_\mu(\mathbf{q},\omega=0,T) \equiv \chi_\mu(\mathbf{q},T)$, the energies $E_{sw}(\mathbf{q})$, and linewidths $\hbar\Gamma_{sw}(\mathbf{q})$ of the spin waves and the linewidth $\hbar\Gamma_z(\mathbf{q})$ of the quasielastic scattering. These quantities will be discussed in the following.

A. Static critical behavior

In order to compare the experimentally determined static susceptibilities with the theory we refer to the expressions from the theoretical work by Schinz and Schwabl¹⁹ who have presented $\chi_\mu(\mathbf{q},T)$ for all \mathbf{q} values and temperatures below T_C . Especially, one finds for the susceptibilities χ_{sw} and χ_z , deep in the dipolar regime as covered by our experiment [Fig. 1(a)],

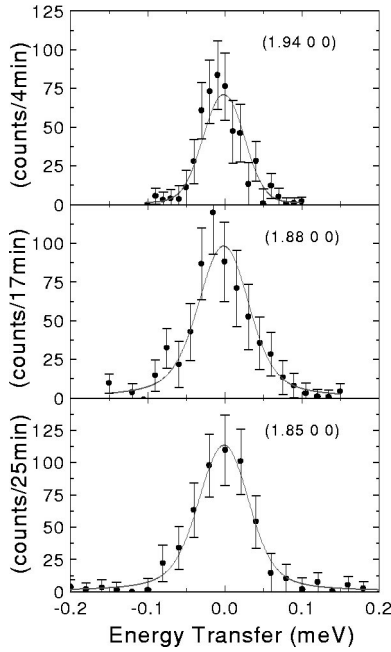


FIG. 5. Spectra of the longitudinal fluctuations recorded at $T = 0.98T_c$ and different momentum transfers \mathbf{q} .

$$\chi_{sw}(\mathbf{q}, T) = \frac{q_d^2}{q^2}, \quad (4)$$

$$\chi_z(\mathbf{q}, T) = \frac{q_d^2}{q^2 + \kappa_-^2(q, T)}. \quad (5)$$

The q^{-2} divergence is characteristic of gapless spin waves with transverse polarization $\delta\mathbf{S}_{sw} \perp \mathbf{q}$, also referred to as Goldstone modes, while the fluctuations parallel to \mathbf{M} acquire a (thermal) mass $\kappa_-^2(T)$. At small momentum transfers $q \ll \kappa_-$, this term is renormalized by the spin-wave fluctuations and becomes \mathbf{q} dependent:

$$\kappa_-^2(q, T) = \frac{29}{18} \frac{\kappa_z^2(T)}{1 + a\kappa_z(T)/q}, \quad (5a)$$

where $\kappa_z = \xi^{-1}$ denotes the inverse correlation length below T_c and $a \approx 2/9$.^{19,26} One consequence of this effect has been emphasized for the homogeneous susceptibility already in the original spin-wave work by Holstein and Primakoff.²⁷ They predicted a singularity for vanishing magnetic field, $\chi_z(q=0, T, B \rightarrow 0) \sim B^{-1/2}$, which in fact has been confirmed in experiments on EuS and EuO.²⁸ More recently, the crossover from the Ornstein-Zernicke-type behavior of the zero-field susceptibility to a $\chi_z(q \ll \kappa_z) \sim q^{-1}$ singularity has been obtained by the RG theory,²⁶ but clear experimental evidence is yet lacking.

A summary of our static results are depicted in Fig. 6(a), where the inverse (ω -integrated) intensities of the spin-flip and non-spin-flip channels measured at five different temperatures are plotted against q^2 . The former turn out to be independent of temperature and display a clearcut q^2 dependence as predicted by Eq. (4) for the spin-wave susceptibility

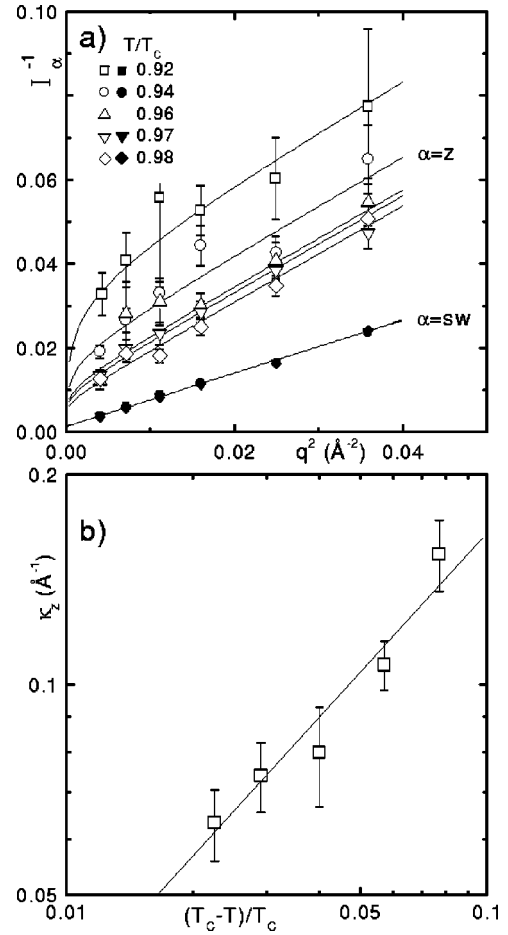


FIG. 6. (a) Inverse of the integrated intensities of the spin-wave and longitudinal spin fluctuations vs q^2 , fitted to the inverse static susceptibilities, $\chi_{sw}^{-1} \sim (q^2 + \kappa_g^2)$ and $\chi_z^{-1}(q \rightarrow 0) \sim [q^2 + \kappa_-^2(T, q)]$, Eq. (5). (b) Temperature dependence of the inverse correlation length of the longitudinal magnetization fluctuations, $\kappa_z(T) = \xi^{-1}(T)$, defined by Eq. (5a).

χ_{sw} . Note that by using a representation of q_d^2 , which involves the spin-wave stiffness $D_{sw}(T)q_d^2 = g_L \mu_B M_s(T)$ [see Ref. 10 and Eq. (7) below] one finds an equivalent form $\chi_{sw}(q \rightarrow 0) = g_L \mu_B M_s(T) / D_{sw}(T) q^2$. In Fig. 6(a), at the lowest q^2 a slight offset is seen, $\chi_{sw}(q=0) = q_d^2 / \kappa_g^2$ with $\kappa_g = 0.04 \text{ \AA}^{-1}$. We ascribe it to the presence of a small gap in the spin-wave spectrum, which may be associated with the small cubic anisotropy of EuS and the finite internal field required to remove the domains.

In contrast to χ_{sw} , the susceptibility of the parallel fluctuations exhibits a strong temperature dependence. Figure 6a displays the fits of the inverse intensities to Eq. (5). At large q^2 , the Ornstein-Zernicke behavior is obeyed which by Eq. (5a) defines the inverse ferromagnetic correlation length $\kappa_z(T) = \sqrt{18/29} \kappa_- (q \gg \kappa_z, T)$, depicted in Fig. 6(b). Obviously, the temperature dependence can be well described by the critical law

$$\kappa_z(T) = \kappa_z(0)(1 - T/T_c)^{\nu'}, \quad (6)$$

with $T_c = 16.25(5) \text{ K}$. The critical exponent $\nu' = 0.68(2)$ agrees with the value obtained above T_c of EuS, ν

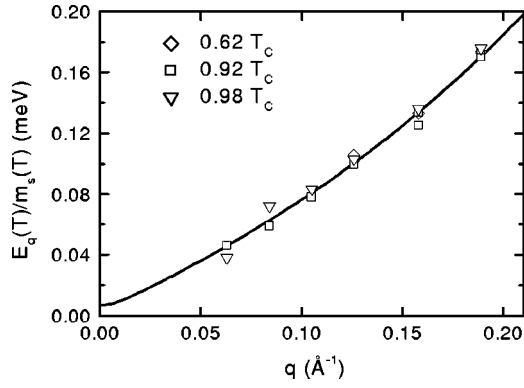


FIG. 7. Dispersion of the spin waves with transverse polarization $\delta S_{sw}^t(\mathbf{q})$ [see Fig. 1(b)]. The energies have been normalized by the reduced spontaneous magnetization $m_s = M_s(T)/M_s(0) = 1.18(1 - T/T_c)^{0.36}$ (Ref. 29) and fitted to the predictions of the Holstein-Primakoff (Ref. 27), Eq. (7).

$= 0.70(2)$,²⁹ as predicted by the static scaling hypothesis. For the critical amplitude we obtain $\kappa_z(0) = 0.91(5) \text{ \AA}^{-1}$. Comparing this value to the amplitude of the paramagnetic correlation length of EuS, $\kappa_p(0) = 0.53 \text{ \AA}^{-1}$,²⁹ we find $\kappa_z = 1.7\kappa_p$, which is bracketed by the mean-field value $\sqrt{2}\kappa(0)$ and $2.02\kappa(0)$ obtained by considering fluctuations.¹⁹

At rather small q , we observe a downward bending of $I_z^{-1}(q)$, which we try to associate with the crossover $\chi_z^{-1}(q \ll \kappa_z) \sim q$ following from Eq. (5a). Though the errors are fairly large, we fitted the inverse intensities to this prediction and found $a = 0.20(5)$, which agrees surprisingly well with $a = 2/9$ predicted by various approaches.^{19,26} Regarding the fact that the temperature variation of this $I^{-1}(q)$ bending is well reproduced, we believe that this constitutes the first signature of the q^{-1} singularity of $\chi_z(q)$ induced by the Goldstone modes. Interestingly, this variation should also hold for the dipolar critical regime.¹⁹

B. Spin-wave dispersion

The spin-wave energies, normalized to the reduced spontaneous magnetization $m_s(T) = M_s(T)/M_s(0) = 1.18(1 - T/T_c)^{0.36}$,^{29,30} are shown in Fig. 7. For the present orientation of \mathbf{q} being perpendicular to \mathbf{M}_s , spin-wave²⁷ and linear response¹⁵ theories predict for the q dependence

$$E(q) = D_0 m_s(T) \tilde{q}^2 \left[1 + \left(\frac{q_d}{\tilde{q}} \right)^2 \right]^{1/2}. \quad (7)$$

As for the static susceptibility we admitted the presence of a small gap $\tilde{q}^2 = q^2 + \kappa_{sw}^2$. Due to the well-known depolarization of one of the precessing components $\delta \mathbf{S}_{sw}$, the dipolar wave number enters Eq. (7) via $q_d^2 \equiv g_L \mu_B M_s(0)/D_0$ to cause a crossover from the quadratic dispersion at $q \gg q_d$ to the linear law for $q_d \gg q > \kappa_{sw}$. The solid line in Fig. 7 represents the fit of the data to Eq. (7) with $D_0 = 3.02 \text{ meV \AA}^2$, $q_d = 0.23(1) \text{ \AA}^{-1}$, and $\kappa_{sw} = 0.01 \text{ \AA}^{-1}$. Comparing this fitted dipolar wave number to $q_d = 0.22(5) \text{ \AA}^{-1}$ as determined from paramagnetic neutron

scattering¹² suggests that this quantity is not renormalized by critical fluctuations when passing T_c . Such an effect has been conjectured by Fisher and Aharony.¹¹ However, some indication for the absence of such renormalizations through critical fluctuations in the dipolar regime has already been realized during a previous determination of q_d .³² There, using the *mean-field* expression for the critical amplitude of the static paramagnetic susceptibility of EuS, $C_0 = [q_d/\kappa_p(0)]^2 = 0.19$,³⁰ $q_d = 0.24(2) \text{ \AA}^{-1}$ was obtained.

We also note that κ_{sw} is smaller by a factor of 4 than κ_g following from the longitudinal susceptibility and the measured value of C_0 . We relate this difference to the dipolar interaction, which invalidates the proportionality $\kappa(q) \sim E_{sw}^{-1}(q)$, as can be inferred from the results of Refs. 16 and 19.

C. Linewidths

The linewidths evaluated here are defined by the Lorentzian shape which we assumed when analyzing the spectra by Eq. (3). Note that already previous studies on powdered EuS (Ref. 3) favored this shape over the Gaussian and the truncated Lorentzian forms. Moreover, also the MMC approach¹⁶ determined the damping of the magnetization modes investigated here by assuming an exponential relaxation at long times, which corresponds to the Lorentzian shape at not too high frequencies.

The results for the widths of the spin-wave peaks and of the central peak of the longitudinal fluctuations are displayed by Fig. 8. Within the experimental errors, there is no temperature variation down to the lowest temperatures in region DC [see shaded area in Fig. 1(a)]. Note that the errors for Γ_z are larger than those for Γ_{sw} because of the smaller spectral weight of the longitudinal fluctuations, as is seen in Fig. 6(a). As the most striking result we infer from the presentations against $q^2 (< q_d^2)$ in Fig. 8 that (i) the relaxation rates of both modes obey the simple relations

$$\Gamma_{sw}(q, T) = L_{sw} \left(\frac{q}{q_d} \right)^2 + \Gamma_{sw}(0, T), \quad (8a)$$

$$\Gamma_z(q, T) = L_z \left(\frac{q}{q_d} \right)^2 + \Gamma_z(0, T), \quad (8b)$$

being indicated as solid lines in Fig. 8, and (ii) that the resulting kinetic coefficients $L_{sw} = 35(2) \text{ \mu eV}$ and $L_z = 40(3) \text{ \mu eV}$ agree within their uncertainties. Moreover, the damping of both modes remains finite with small values of this background damping, $\Gamma_{sw}(0, T) = 0.6(4) \text{ \mu eV}$ and $\Gamma_z(q=0) = 2.8(4) \text{ \mu eV}$, which will also be discussed in the next section.

V. DISCUSSION

We start from a rather general aspect of the critical phenomena, i.e., the scaling hypothesis extended to dynamical quantities, like the relaxation rate of the order parameter.⁵ Then the dipolar interaction in Heisenberg ferromagnets can fully be taken into account by introducing q/q_d as a second

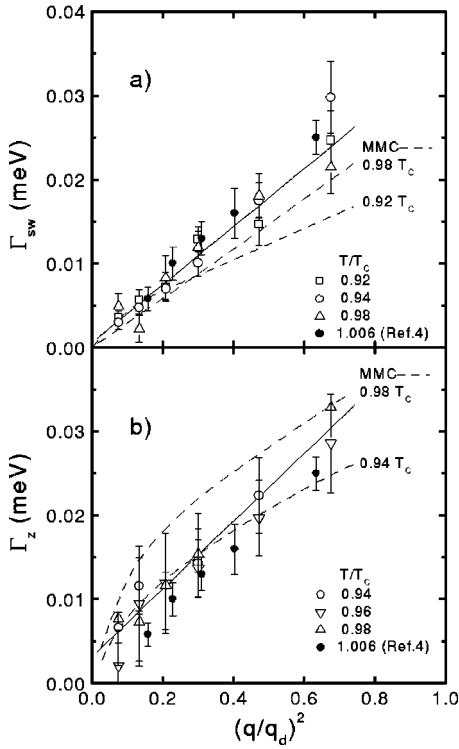


FIG. 8. q dependence of the Lorentzian linewidths of the (a) spin waves and (b) longitudinal fluctuations at selected temperatures measured in the dipolar critical regime; see Fig. 1(a). For comparison are indicated data taken on powdered EuS at $T = T_C$.

scaling variable^{14,16} in the homogeneous scaling function g_μ for the linewidths of the transverse modes investigated here [see Fig. 1(b)]:

$$\Gamma_\mu^t(q, T) = q^z g_\mu \left(\frac{q}{\kappa_\mu}, \frac{q}{q_d} \right). \quad (9)$$

Let us first approach the problem from the *paramagnetic* side to which we designate the index $\mu = p$. There according to both experiment⁷ and MMC theory¹³ the crossover from exchange-dominated dynamics, being characterized by the exponent $z = (D + 2)/2 = 5/2$, to the dipolar critical dynamics with $z = 2$ occurs deep in the DC region, i.e., for $q, \kappa(T) \ll q_d$. This is the reason why dipolar effects were not realized in the early investigations.¹⁻⁴ Once the dipolar dynamics, i.e., $z = 2$, has taken over very close to T_C , where $\kappa_p(T) \ll q_d$, the paramagnetic scaling function assumes a constant value [see Eq. (7) of Ref. 18]:

$$g_p(\infty, 0) = L_d q_d^{-2}. \quad (10)$$

For EuS, the (dipolar) kinetic coefficient L_d has been determined from analysis of the relaxation rates of the transverse fluctuations in the limit $q \rightarrow 0$ above²⁰ and below T_C (Ref. 31):

$$\Gamma_p^t(q \rightarrow 0, T) = \frac{L_d}{\chi_p^t(q \rightarrow 0)}. \quad (11)$$

The value $\hbar L_d = 38(4) \mu\text{eV}$ was found to agree fairly well with the MMC estimate^{13,14,18} $\hbar L_d = 5.1 g_L \mu_B \sqrt{k_B T_C / \mu_0} q_d^{3/2} / 4\pi^2 \approx 30 \mu\text{eV}$.

Below T_C , as a matter of fact, we recover here the same q^2 dependence of both relaxation rates Γ_z and Γ_{sw} , Eq. (8), and in particular, within the experimental errors, their coefficients agree with L_d , $L_{sw} \approx L_z \approx L_d$. These are the central results of our work. In terms of the dynamical scaling hypothesis they imply that by passing the Curie temperature from above, the dipolar dynamic universality class for the transverse (critical) fluctuations $\delta\mathbf{S}^t$ characterized by $z = 2$ is not changed. This basic feature is nicely confirmed by (rather old) $\Gamma_p^t(q)$ data measured slightly above T_C of powdered EuS, which we have added to Fig. 8(a). Within the given error bars, they agree with respect to the magnitude and q^2 variation with the present Γ_{sw}^t data taken below T_C . We also observe a slight systematic enhancement of $\Gamma_z^t(q, T < T_C)$ over $\Gamma_p^t(q, T_C)$, which seems to be associated with the (small) background $\Gamma_{z,bg}$ to be discussed below.

To date, the fundamental phenomenon of dynamical scaling in Heisenberg ferromagnets has been established for the exchange (“true”)critical regime [EC in Fig. 1(a)], i.e., for $q > \kappa(T) > q_d$, where Γ^t becomes independent of temperature; i.e., $\Gamma^t \sim (q/q_d)^{5/2}$ is maintained on both sides of T_C .^{1-4,18} Our experiment provides evidence for the “true” (temperature-independent) dipolar critical behavior extending to even smaller q values, $q < \kappa_z(T)$; see shaded region in Fig. 1(a). A temperature variation might set in when the DH is reached. This extended *dynamic* critical behavior with $z = 2$ below T_C is also very much different from the situation above T_C , where $z = 2$ is attained for extremely small $q \ll q_d$,^{7,13} and only a small part of the static DC region is occupied by *dynamic* dipolar criticality. Both features are consistent with the general fact that the dynamic critical behavior reflects more details of the system, in particular conservation laws,⁵ than static properties, like the susceptibility tensor $\tilde{\chi}(\mathbf{q})$, which define the critical regimes displayed in Fig. 1(a).

Having established the dynamic class $z = 2$ in a large part of the DC regime below T_C , we are now able to discuss the further consequences of the q variation of the damping, Eq. (8). The kinetic coefficients L_z and L_{sw} turned out to be identical for both the spin-wave and the longitudinal modes. By looking at Fig. 1(b), this result emerges from the continuity of the critical behavior of the transverse modes $\delta\mathbf{S}^{t1}(\mathbf{q})$ and $\delta\mathbf{S}^{t2}(\mathbf{q})$. Note that above T_C , the designations “transverse” and “longitudinal” define orientations of $\delta\mathbf{S}$ with respect to \mathbf{q} , being indicated by a superscript in $\delta\mathbf{S}^\alpha$. Below T_C , due to the symmetry breaking through $M_s \mathbf{e}_z$, this “conventional” definition of the mode polarization $\delta\mathbf{S}(\mathbf{q})$ is possible only for certain \mathbf{q} directions, like the one chosen in the present work. The transverse modes drive the ferromagnetic transition on the paramagnetic side, where the \mathbf{q} vector clearly determines the symmetry. By passing T_C from above, Fig. 1(b) suggests the continuous transformations $\delta\mathbf{S}^{t1} \rightarrow \delta\mathbf{S}_{sw}^t$ and $\delta\mathbf{S}^{t2} \rightarrow \delta\mathbf{S}_z^t$. Note that this is only true for our experimental configuration, where the order parameter \mathbf{M}_s is oriented perpendicular to \mathbf{q} . The fact that the kinetic coeffi-

cients below T_C , L_{sw} , and L_z are equal and, moreover, agree with $L_p = 38(2) \mu\text{eV}$ of $\delta\mathbf{S}'(\mathbf{q})$ above T_C (Refs. 4 and 18) (see also Fig. 8) can be immediately be related to the modes with transverse polarization $\delta\mathbf{S}_\perp \mathbf{q}$, which are the only ones to become critical in real Heisenberg ferromagnets, i.e., with dipolar interaction. On the paramagnetic side, these critical modes display relaxational dynamics, but below T_C their dynamical shape depends on the direction of their propagation vector with respect to the order parameter \mathbf{M}_s . If these transverse critical modes propagate, for example, along \mathbf{M}_s , they are predicted to exhibit spin-wave dynamics in DC (Refs. 15 and 16) with pure Goldstone-like susceptibilities $\chi_{sw}^t(\mathbf{q} \parallel \mathbf{M}_s) = (q_d/q)^2$.¹⁹ The remaining longitudinal mode $\delta\mathbf{S}_z \parallel \mathbf{q}$ should be strongly damped and suppressed in intensity. These modes can be studied in a configuration, where the polarizing field \mathbf{B} is oriented parallel to the scattering plane.

The dipolar symmetry with respect to \mathbf{q} is also reflected by the fact that in the DC regime the direction of \mathbf{q} is parallel to the largest eigenvector of the susceptibility tensor $\tilde{\chi}(\mathbf{q})$,¹⁸ \mathbf{v}_3 , while the second largest, \mathbf{v}_2 , is parallel to \mathbf{M}_s . This symmetry of $\tilde{\chi}(\mathbf{q})$ changes if the DC regime is left. Then the directions of these two eigenvectors are just interchanged for our configuration $\mathbf{q} \perp \mathbf{M}_s$, while for a general orientation between \mathbf{q} and \mathbf{M}_s a gradual rotation, $\mathbf{v}_3 \rightarrow \mathbf{v}_2$ and $\mathbf{v}_2 \rightarrow -\mathbf{v}_3$, takes place. Hence, outside of the DC regime, the “leading” static symmetry of the ferromagnet is defined by the order parameter \mathbf{M}_s and, moreover, the dynamical exponent attains its isotropic value, $z = 5/2$. This implies that there both spin-wave modes $\delta\mathbf{S}_{sw\perp}^t \mathbf{q}$ and $\delta\mathbf{S}_{sw\parallel}^t \mathbf{q}$ are critical. Recently, their frequencies have been investigated in some detail by polarized neutrons.²¹ For the damping similar data are still lacking. Early work employing unpolarized neutrons³ away from T_C of EuO provided relaxation rates, which were consistent with $\Gamma_{sw}(q, T) \sim \kappa_z^{-3/2} q^4$. This agrees with the scaling hypothesis, Eq. (9), provided $g_{sw} = [q/\kappa_z(T)]^{3/2} \tilde{g}_{sw}(0, \infty)$. Unlike our observation in the DC region, in the exchange critical regime the dominance of the thermally excited spin waves gives rise to the strong increase of their linewidths with temperature. The leading q^4 dependence has been predicted by Vaks *et al.*³³ and results from spin-wave–spin-wave scattering.

Another interesting point is the fact that both linewidths do not change with temperature down to the lowest values studied here, $T/T_C = 0.92$. This is somewhat surprising with regard to the existing results of the MMC calculations,^{16,34} which using some interpolation have also been indicated in Fig. 8. We notice that they predict a slight temperature variation, i.e., a narrowing with decreasing T , which is not observed. Also the q^2 variations of our linewidths are not reproduced and the absolute MMC values for Γ_{sw} and Γ_z are smaller and larger, respectively. This seems to indicate that the assumptions of the MMC approach, like the Lorentzian approximation for the modes with large q and some cutoff of the dynamics, may not be valid. By a more phenomenological point of view, we rather conjecture that the noncritical longitudinal fluctuations $\delta\mathbf{S}_z \parallel \mathbf{q}$ play a much more important role than believed to date. Their damping is expected to be

$\Gamma_z^l(q) = L_d/\chi_z^l = L_d$, i.e., temperature independent and rather large, and may provide an efficient relaxation channel for the critical modes. The importance of Γ_z^l has been realized recently in the relaxation rate of the homogeneous magnetization Γ_z^l below T_C .³¹

A final comment on the “background” damping of the longitudinal fluctuations, $\Gamma_z(q=0, T \leq T_C) = 2.8 \mu\text{eV}$, may be appropriate. We conjecture here that—similarly as above T_C (Ref. 18)—damping effects by the longitudinal polarization of the $\delta\mathbf{S}_z^l$ mode are picked up within the resolution of our experiment. Due to the dipolar demagnetization, these modes are uncritical [dynamic exponent $z=0$ (Ref. 14)]. This conjecture is based on the fact that our background value is rather close to $\Gamma_{z,bg} = L_{bg}/\chi_z^l(q=0, T \leq T_C) = 1.8(2) \mu\text{eV}$, where we have inserted (i) the background kinetic coefficient $L_{bg} = 1.8(2) \mu\text{eV}$, determined from the critical behavior of $\Gamma^l(q=0, T > T_C)$,¹⁸ and (ii) the susceptibility of the longitudinal spin-wave modes, $\chi_{sw}^l(q \rightarrow 0, T < T_C) = 1$, which at $T = T_C$ transform into the longitudinal paramagnetic modes $\chi^l(q \rightarrow 0)$. It may be interesting to note that this background seems to be absent or at least significantly be reduced in the paramagnetic relaxation rate $\Gamma_p^l(q, T)$ of Ref. 4, depicted in Fig. 8. This indicates that the appearance of the order parameter increases $\Gamma_z^l(0, T)$ while its effect on the background rate of the spin-wave linewidth, $\Gamma_{sw}^l(0, T) = 0.5(4) \mu\text{eV}$, turns out to be small.

VI. SUMMARY AND CONCLUSIONS

We have conducted a study of the dynamics of spin fluctuations in the ferromagnetic state of EuS close to T_C , where dipolar effects are expected to play a dominant role. For intensity reasons we concentrated on the spin-wave and longitudinal fluctuations $\delta\mathbf{S}_{sw}^t$ and $\delta\mathbf{S}_z^t$, both transverse with respect to the momentum transfer \mathbf{q} , which was chosen perpendicular to \mathbf{M} . This configuration allowed us to extract from the spin-wave frequencies the characteristic dipolar wave number q_d and from the static susceptibility $\chi_z(\mathbf{q}, T)$ the correlation length $\xi_z = \kappa_z^{-1}$ of the longitudinal fluctuations. The latter exhibits deviations from the Ornstein-Zernicke law at $q \ll \kappa_z$, which appear to be related to the predicted thermal renormalization of χ_z by the spin waves.^{26,16} This feature, though the subject of rather intense research in the past years (see, e.g., Refs. 35–37), has not been identified before. The reason for the observation of the mass renormalization of $\chi_z(\mathbf{q}, T)$ on EuS can be attributed to the rather large critical amplitude $\kappa_z(0) = 0.91 \text{ \AA}^{-1}$, which allows us to explore the regime $q/\kappa_z \ll 1$. This is in contrast to the situation in the itinerant ferromagnet Ni,³⁶ where $\kappa_z(0)$ is almost one order of magnitude smaller.

As the central result of our study, we regard the linewidths of both modes. They display the same \mathbf{q} variation $\Gamma_\mu = L_d(q/q_d)^2$, which we explained by using the dynamical scaling hypothesis and existing data for $\Gamma^l(\mathbf{q}, T \geq T_C)$ of EuS. Apart from a small finite background for $\Gamma_z(q=0)$, which was already observed above T_C in a previous work, the absolute values of both linewidths prove to be identical. Moreover, the relevant kinetic coefficient L_d agrees with the

value obtained from the linewidths of the transverse fluctuations $\delta\mathbf{S}_p^t(\mathbf{q})$ measured in the dipolar critical regime slightly above T_C . This quantitative feature suggests the transformations $\delta\mathbf{S}_p^t \rightarrow \delta\mathbf{S}_{sw}^t$ and $\delta\mathbf{S}_p^t \rightarrow \delta\mathbf{S}_z^t$ when passing T_C from the para- to the ferromagnetic side without any change of the dynamics and thus obeying dynamical scaling—as conjectured in Ref. 22. As a surprising feature we note that the “true,” i.e., temperature-independent, dipolar critical behavior extends so far into the static DC region explored here; see Fig. 1(a). This is in contrast to the extremely narrow regime just above T_C , in which the dipolar anisotropy changes the dynamic universality class of the transverse modes from $z = 5/2$ to $z = 2$. The observed q and temperature variations of our linewidths are not fully consistent with predictions by the MMC theory,¹⁶ which is a bit unexpected regarding the success of this approach on the paramagnetic side.^{14,15}

Finally we should note that for intensity reasons we were not yet able to measure the crossover of Γ_z^t to the hydrodynamic ($q < \kappa_z/9$) and to the exchange critical ($q > q_d$) regime, for which some more theoretical work has been published.^{38,39,26,33,14} An even greater experimental challenge is the low intensity of the longitudinal polarizations $\delta\mathbf{S}_{sw}^t$ ²² and $\delta\mathbf{S}_z^t$. Their noncritical dynamics may be responsible for the absence of any temperature effects on the both linewidths investigated here. Other unsettled problems are the mechanisms responsible for the small and noncritical background effects occurring in the static susceptibilities, spin-wave frequencies, and relaxation rates. The values quoted here for $\kappa_g, \kappa_{sw}, \Gamma_z(0, T)$, and $\Gamma_{sw}^t(0, T)$ may help to answer the question as to whether there exists a common origin, like anisotropy or finite internal magnetic field.

*Electronic address: koetzler@physnet.uni-hamburg.de

¹M.F. Collins, V.J. Minkiewicz, R. Nathans, L. Passell, and G. Shirane, *Phys. Rev.* **179**, 417 (1969).

²V.J. Minkiewicz, M.F. Collins, R. Nathans, and G. Shirane, *Phys. Rev.* **182**, 624 (1969).

³O.W. Dietrich, J. Als-Nielsen, and L. Passell, *Phys. Rev. B* **14**, 4923 (1976).

⁴P. Böni, G. Shirane, H.G. Bohn, W. Zinn, *J. Appl. Phys.* **61**, 3397 (1987).

⁵B.I. Halperin and P.C. Hohenberg, *Phys. Rev.* **177**, 952 (1969); P.C. Hohenberg and B.I. Halperin, *Rev. Mod. Phys.* **49**, 435 (1977).

⁶J. Kötzler and H.v. Philipsborn, *Phys. Rev. Lett.* **40**, 790 (1978).

⁷F. Mezei, *Phys. Rev. Lett.* **49**, 1096 (1982).

⁸D.L. Huber, *J. Phys. Chem. Solids* **32**, 2145 (1971); R. Raghavan and D.L. Huber, *Phys. Rev. B* **14**, 1185 (1976).

⁹W. Finger, *Phys. Lett.* **60A**, 165 (1977).

¹⁰J. Kötzler, *Phys. Rev. Lett.* **51**, 833 (1983).

¹¹M.A. Fisher and A. Aharony, *Phys. Rev. Lett.* **30**, 559 (1973).

¹²J. Kötzler, F. Mezei, D. Görlitz, and B. Farago, *Europhys. Lett.* **1**, 675 (1986).

¹³E. Frey and F. Schwabl, *Z. Phys. B: Condens. Matter* **71**, 355 (1988).

¹⁴E. Frey and F. Schwabl, *Adv. Phys.* **43**, 577 (1994).

¹⁵H. Schinz and F. Schwabl, *Phys. Rev. B* **57**, 8438 (1998).

¹⁶H. Schinz and F. Schwabl, *Phys. Rev. B* **57**, 8456 (1998).

¹⁷P. Böni, D. Görlitz, J. Kötzler, and J.L. Martínez, *Phys. Rev. B* **43**, 8755 (1991).

¹⁸J. Kötzler, *Phys. Rev. B* **38**, 12 027 (1988).

¹⁹H. Schinz and F. Schwabl, *Phys. Rev. B* **57**, 8430 (1998).

²⁰J. Kötzler, G. Kamleiter, and G. Weber, *J. Phys. C* **9**, L361 (1976).

²¹P. Böni, M. Hennion, and J.L. Martínez, *Phys. Rev. B* **52**, 10 142 (1995).

²²P. Böni, B. Roessli, D. Görlitz, J. Kötzler, and J.L. Martínez (unpublished).

²³S.W. Lovesey, *Theory of Neutron Scattering from Condensed Matter* (Clarendon Press, Oxford, 1984), Vol. 2.

²⁴The energy independent background of 1 count/8.3 min seems to be unreasonably small. The reason is that the fitted spectral weight functions were approximated by Lorentzians that usually enforce a too low background when fitting data as discussed in Ref. 25.

²⁵P. Böni, M.E. Chen, and G. Shirane, *Phys. Rev. B* **35**, 8449 (1987).

²⁶G. Mazonko, *Phys. Rev. B* **14**, 3933 (1976).

²⁷T. Holstein and H. Primakoff, *Phys. Rev.* **58**, 1098 (1940).

²⁸J. Kötzler, D. Görlitz, R. Dombrowski, and M. Pieper, *Z. Phys. B: Condens. Matter* **94**, 9 (1994).

²⁹J. Als-Nielsen, O.W. Dietrich, and L. Passell, *Phys. Rev. B* **14**, 4908 (1976).

³⁰J. Kötzler and M. Muschke, *Phys. Rev. B* **34**, 3543 (1986).

³¹D. Görlitz and J. Kötzler, *Eur. Phys. J. B* **5**, 37 (1998).

³²J. Kötzler, *J. Magn. Magn. Mater.* **54-57**, 649 (1986).

³³V.G. Vaks, A.I. Larkin, and S.A. Pikin, *Sov. Phys. JETP* **26**, 188 (1968).

³⁴H. H. W. Schinz, Ph. D. thesis, Technical University of Munich, 1994.

³⁵P.W. Mitchell, R.A. Cowley, and R. Pynn, *J. Phys. C* **17**, L875 (1984).

³⁶P. Böni, J.L. Martínez, and J.M. Tranquada, *Phys. Rev. B* **43**, 575 (1991).

³⁷R. Coldea, R.A. Cowley, T.G. Perring, D.F. McMorrow, and B. Roessli, *Phys. Rev. B* **57**, 5281 (1998).

³⁸R. Résibois and C. Piette, *Phys. Rev. Lett.* **24**, 514 (1970).

³⁹S.V. Maleev, *Sov. Sci. Rev., Sect. A* **8**, 323 (1987).